Article

A New Mechanism for Cement Hydration Inhibition: Solid-State Chemistry of Calcium Nitrilotris(methylene)triphosphonate

Maximilienne Bishop, Simon G. Bott, and Andrew R. Barron

Chem. Mater., **2003**, 15 (16), 3074-3088 • DOI: 10.1021/cm0302431

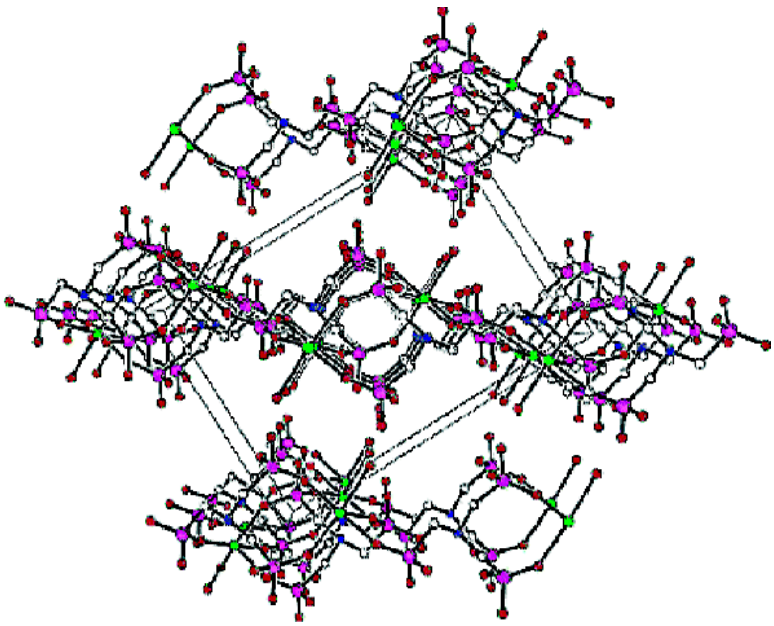

A New Mechanism for Cement Hydration Inhibition: Solid-State Chemistry of Calcium Nitrilotris(methylene)triphosphonate

Maximilienne Bishop,[†] Simon G. Bott,[‡] and Andrew R. Barron*,[†]

Department of Chemistry and Center for Nanoscale Science and Technology, Rice University, Houston, Texas 77005, and Department of Chemistry, University of Houston, Houston, Texas 77204

Received February 28, 2003. Revised Manuscript Received May 27, 2003

The reaction of the cement retarder nitrilo-tris(methylene)phosphonic acid, $N[CH_2PO(OH)_2]_3$ (H_6ntmp) with calcium oxide, tricalcium silicate (C3S), tricalcium aluminate (C3A), and tetracalcium aluminoferrite (C4AF) has been studied individually, and in the case of C3A in the presence of gypsum, to gain an understanding of the effect on the individual minerals prior to studying a typical sample of Portland cement. The reaction of H_6ntmp with calcium oxide results in the initial formation of soluble $[Ca(H_n\text{ntmp})]^{(4-n)-}$, which precipitates over time as $[Ca(H_4\text{ntmp})(H_2O)]_\infty$, whose sheetlike structure has been confirmed by single-crystal X-ray diffraction. The study of the hydration of C3S in the presence of H_6ntmp indicates that no C−S−H forms, and the surface changes from silicon-rich to calcium-rich associated with the formation of various calcium phosphonates. The hydration of C3A is severely inhibited in the presence of H_6ntmp, with the phosphonic acid reacting primarily with calcium as opposed to aluminum to form a Ca−P-rich layer at the surface of C3A. The H_6ntmp enhances calcium solubility, promoting the dissolution of calcium from C3A and promoting, in the presence of gypsum, the formation of ettringite. In the presence of H_6-ntmp the surface of hydrated Portland cement grains is rich in calcium and phosphorus and deficient in silicon and aluminum, consistent with the formation of a calcium phosphonate coating spectroscopically related to $[Ca(H_4\text{ntmp})(H_2O)]_\infty$. We have proposed a new mechanism by which phosphonic acids inhibit cement hydration. Dissolution, of calcium by extraction with the phosphonic acid, exposes the aluminum-rich surface to enhance hydration, followed by precipitation of a layered calcium phosphonate that binds to the surface of the cement grains, inhibiting further hydration by acting as a diffusion barrier to water as well as a nucleation inhibitor. Samples were characterized by ^{31}P, ^{27}Al, and ^{29}Si MAS NMR spectroscopy, scanning electron microscopy, X-ray diffraction, and X-ray photoelectron spectroscopy.

Introduction

Cementitious materials have been in use for over 2000 years and to this day are considered essential to both the construction and oil industries. Portland cement, in particular, has found success in a wide range of applications due to its unique hardening process. The addition of water to dry cement powder results in a thin cement slurry that can be easily manipulated and cast into different shapes. In time, the slurry sets and develops strength through a series of hydration reactions.[1] Hydration of cement is not linear through time; it proceeds very slowly at first, allowing the thin mixture to be properly placed before hardening. Despite their mundane and low-tech status, cements and the cementation process are not well understood due to the complex nature of the number and interdependence of the chemical reactions.

Portland Cement is manufactured by heating calcium carbonate and clay or shale to 1450 °C. The calcium carbonate is converted to calcium oxide, or lime, and the clay minerals yield dicalcium silicate (Ca_2SiO_4, C2S)[2] and other inorganic oxides such as aluminates and ferrites. Further heating melts the aluminate and ferrite phases. The lime reacts with dicalcium silicate to from tricalcium silicate (Ca_3SiO_5, C3S). As the mixture is cooled, tricalcium aluminate ($Ca_3Al_2O_6$, C3A), and tetracalcium aluminoferrite ($Ca_4Al_nFe_{(2-n)}O_7$, C4AF) crystallize from the melt and tricalcium silicate and the remaining dicalcium silicate undergo phase transitions.[1] These four minerals comprise the bulk of most cement mixtures.[2]

* To whom correspondence should be addressed. E-mail: arb@rice.edu. URL: www.rice.edu/barron.
† Rice University.
‡ University of Houston.

(1) Taylor, H. F. W. *Cement Chemistry, 2nd Ed.*; Academic Press: London, 1997.

(2) Each of the minerals, Ca_2SiO_4, Ca_3SiO_5, $Ca_3Al_2O_6$, and $Ca_4Al_nFe_{(2-n)}O_7$, can be conceptually broken down into the basic calcium, silicon, aluminum, and iron oxides (CaO, SiO_2, Al_2O_3, and Fe_2O_3, respectively) and hence the traditional cement nomenclature abbreviates each oxide, C2S, C3S, C3A, and C4AF. For consistency with the industry nomenclature, we will use the component formulation [i.e., $(CaO)_3(SiO_2)$] rather than the chemical formula (i.e., Ca_3SiO_5).

10.1021/cm0302431 CCC: $25.00
Published on Web 07/09/2003

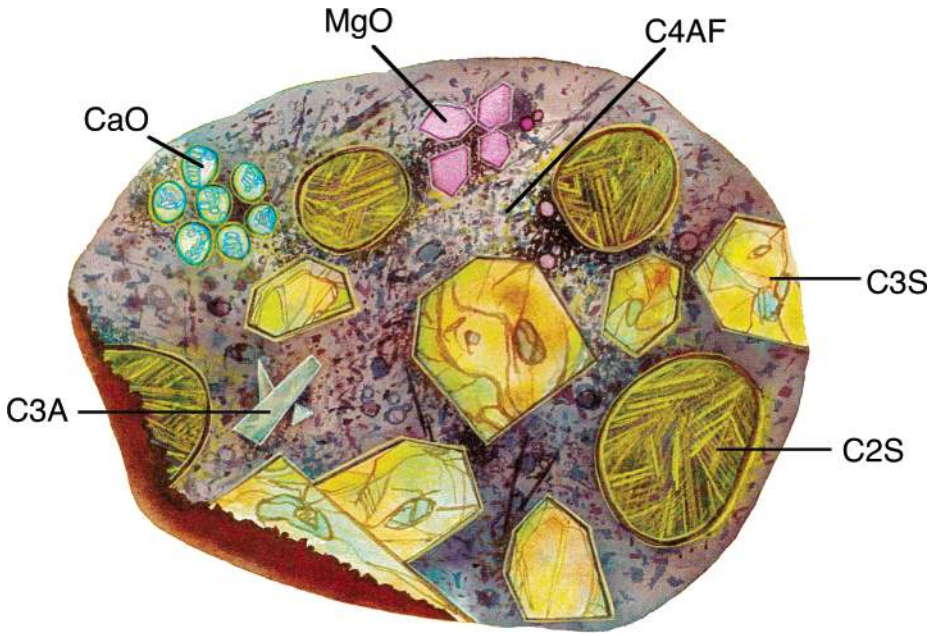

Figure 1. A pictoral representation of a cross section of a cement grain. Adapted from *Cement Microscopy*; Halliburton Services: Duncan, OK.

In the oil industry, bore holes of ever-increasing depths are supported by Portland cement. This application requires a high degree of control over the setting kinetics to allow the cement to be pumped down in a liquid form. A number of chemicals are employed to delay the setting time. Recent work has concentrated on a series of organic phosphonic acids, in particular, nitrilo-tris(methylene)phosphonic acid, $N[CH_2PO(OH)_2]_3$ (**I**, H_6ntmp).[3] The phosphonic acids have been termed

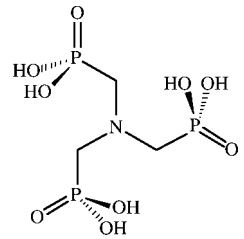

(**I**)

"super retarders" due to their increased effect on cement hydration relative to the effect of conventional retarders.[1,3] The ability of phosphonic acids to retard cement setting by lengthening the induction period, but not slowing down the time it takes for setting to occur (once the acceleratory period has begun), makes them especially interesting candidates for study.[4] The chemical reactions that cause the delay in hardening are not completely understood; however, they are critical to developing a rational methodology for the control of cement setting.

Phosphonic acids are known to complex calcium and other M^{2+} cations,[5] poison the nucleation and growth of barium sulfate crystals,[6] and inhibit the hydration of Fe_2O_3 and Al_2O_3 surfaces via direct surface adsorption.[7] These processes fall into three of the four primary models for cement hydration inhibition: calcium complexation, surface adsorption, nucleation poisoning, and protective coating.[1] There have been a number of previous investigations into the action of phosphonic acids in cement. Ramachandran et al. found that the number of PO_3 groups on the phosphonic acid influenced the effectiveness as a retarder.[8] The same study also found that the phosphonic acids were slightly more effective than the corresponding phosphonates; however, no precise mechanism of inhibition was proposed. In a separate series of studies, a model of the kinetics of cement hydration in the presence of phosphonic acids was developed in which it was assumed that the phosphonic acid residues inhibited the crystallization of gelatinous ettringite by adsorbing onto the surface of the grains.[9]

The hydration of cement is obviously far more complex than the sum of the hydration reactions of the individual minerals. Figure 1 depicts a typical cement grain, showing the larger C2S and C3S particles surrounded by the much smaller C3A and C4AF matrix. In our present study, the reactions of H_6ntmp with C3S and C3A were studied individually to gain an understanding of the effects on the individual minerals prior to studying a typical sample of Portland cement. In addition, the product from the reaction of H_6ntmp with calcium oxide (and hydroxide) has been characterized to provide a comparative model system.

As a result of our investigation, we propose a new mechanism for cement inhibition: "dissolution−precipitation".

(3) Childs, J. D.; Sutton, D. L.; Sabins, F. L. U.S. Patent 4,676,-832, 1987.
(4) Coveney, P.; Davey, R.; Griffin, J.; Whiting, A. *J. Chem. Soc., Chem. Commun.* **1998**, 1467.
(5) Sawada, K.; Duan, W.; Ono, M.; Satoh, K. *J. Chem. Soc., Dalton Trans.* **2000**, *6*, 919.
(6) Benton, W.; Collins, I.; Grimsey, I.; Parkinson, G.; Rodger, S. *Faraday Discuss.* **1993**, *95*, 281.
(7) (a) Davis, G.; Ahearn, J.; Venables, J. *J. Vac. Sci. Technol.* **1984**, *2*, 763. (b) Davis, G.; Ahearn, J.; Matienzo, L.; Venables, J. *J. Mater. Sci.* **1985**, *20*, 975.
(8) Ramachandran, V.; Lowery, M.; Wise, T.; Polomark, G. *Mater. Struct.* **1993**, *20*, 425.
(9) (a) Coveney, P.; Humphries, W. *J. Chem. Soc., Faraday Trans.* **1996**, *92*, 831. (b) Wattis, J.; Coveney, P. *J. Chem. Phys.* **1997**, *106*, 9122. (c) Griffin, J.; Coveney, P.; Whiting, A.; Davey, R. *J. Chem Soc., Perkin Trans.* **1999**, *2*, 1973.

Experimental Section

Samples of tricalcium silicate (C3S) and tricalcium aluminate (C3A) were obtained from Construction Technology Laboratories, Inc., Skokie, IL. Class H Portland Cement and cement clinkers were provided by Halliburton Energy Services, Duncan, OK. All samples were used as received and stored in a desiccator to reduce hydration and carbonation in air. Nitrilotris(methylene)phosphonic acid (H_6ntmp) was purchased from Aldrich chemicals as a 50 wt % aqueous solution and used without further purification. A sample of the H_6ntmp containing retarder, Dequest 2000, was provided by Halliburton Energy Services. Characterization by solution ^{31}P NMR and ^{31}P MAS NMR spectroscopies showed three major impurities, [$RCH_2P(O)(OH)_2$], H_3PO_4, and $HP(O)(OH)_2$. However our analysis revealed that H_6ntmp is the most reactive species in cement pastes.[10] SEM images were observed on a Philips XL-30 ESEM. The samples were attached to a glass slide using carbon tape and then sputtered with gold to reduce charging effects. Powder X-ray diffraction studies were performed on a Siemens diffractometer. XPS analysis was performed at the University of Houston on a PHI 5700 ESCA system with a 1-mm omni focus lens area, an aluminum anode at 400 W, 27−28 mA, and a base pressure of 10^{-10} Torr.

NMR Spectroscopy. Solid state ^{29}Si MAS NMR spectra were observed at 39.8 MHz on a Bruker Avance 200 spectrometer using a VTN probe designed for use with a 7-mm o.d. ZrO_2 rotor. A MAS spin rate of 5 kHz was employed. Samples were studied using a 5.5-μs pulse based on 90° pulse width calibrations with hexamethylcyclotrisiloxane. Chemical shifts were referenced to hexamethylcyclotrisiloxane at $\delta = -10.9$ ppm. Spectra were collected with a 30−60-s acquisition delay. FIDs were processed with 5-Hz line broadening.

Solid state ^{27}Al MAS NMR spectra were obtained at 52.1 MHz on a Bruker Avance 200 spectrometer equipped with two probes designed for use with 7- and 4-mm o.d. ZrO_2 rotors. Samples were studied using 0.5- and 0.3-μs pulses for the 7- and 4-mm probes, respectively, based on 90° pulse width calibrations with solid aluminum nitrate. MAS spin rates of 5 kHz (7-mm rotor) and 9-kHz (4-mm rotor) were used. Spectra were collected with a 0.1−1.0-s acquisition delay. FIDs were processed with 50-Hz line broadening. Samples were externally referenced to the peak maximum of solid aluminum nitrate at $\delta = -1.9$ ppm. The shift of solid aluminum nitrate on this instrument was found by using an external reference of 1.0 M aqueous aluminum nitrate at $\delta = 0.0$ ppm. Solid state ^{27}Al MAS NMR spectra at 130.3 MHz were obtained on a Bruker Avance 500 spectrometer designed for use with a probe equipped with a 2.5-mm o.d. ZrO_2 rotor. Spectra were studied using a 0.3-μs pulse based on 90° pulse width calibrations with solid aluminum nitrate. A MAS spin rate of 33333 Hz was used. Spectra were collected with a 0.5-s acquisition delay. FIDs were processed using 13-Hz line broadening.

Solid state ^{31}P MAS NMR spectra were obtained at 81.0 MHz on a Bruker Avance 200 spectrometer using a VTN probe designed for use with a 7-mm rotor. Samples were studied using a 3.0-μs pulse based on 90° pulse width calibrations with $NH_4{\cdot}H_2PO_4$. Spectra were collected with an 8.0-s relaxation delay and a MAS spin rate of 5 kHz. Proton-coupled spectra were collected using a 0.3-s FID acquisition time. High-power proton-decoupled spectra were collected using only a 35-ms FID acquisition time. The samples were externally referenced to $NH_4{\cdot}H_2PO_4$ at 1.0 ppm.[11] Solution ^{31}P NMR spectra were obtained on a Bruker Avance 400 spectrometer at 161.9 MHz. Spectra were collected using a 6-μs pulse based on 90° pulse width calibrations with 85% phosphoric acid and a 2-s relaxation delay.

Hydration Reactions. Hydration reactions were performed using freshly boiled and cooled deionized water inside a nitrogen-filled glovebag in the presence of ground LiOH to avoid CO_2 contamination. All hydration reactions were carried out at room temperature, typically 22−25 °C. No attempt was made to compensate for the exothermic nature of the reactions.

Tricalcium silicate (C3S) (1.0 g, 4.4 mmol) and water (0.3−0.45 mL) were added to a plastic vial and stirred with a metal spatula for ca. 20 s. For ^{29}Si MAS NMR investigations, 0.45 mL of water was used and hydration was allowed to continue for up to 2 weeks. For SEM studies, C3S samples were hydrated with 0.3 mL of water for 24 h and 2 weeks.

Tricalcium aluminate (C3A) (1.0 g, 3.7 mmol) and water (0.3 mL) were added to a plastic vial and stirred with a metal spatula for ca. 20 s. Samples for ^{27}Al MAS NMR investigations were hydrated inside the N_2 bag and then immediately packed into ZrO_2 rotors to allow for in situ observation of aluminate hydration. Samples for SEM were hydrated for 4 h prior to analysis. The high-vacuum gold sputtering conditions were sufficient to halt hydration.

Studies on C3A hydration in the presence of excess gypsum were performed by mixing C3A (0.6 g, 2.2 mmol) and $CaSO_4{\cdot}2H_2O$ (0.4 g, 2.3 mmol) and then hydrating with water (0.3 mL) and stirring for ca. 20 s. Samples for ^{27}Al MAS NMR investigations were hydrated inside the N_2 bag and then immediately packed into ZrO_2 rotors to allow for in situ observation of ettringite formation. Samples for SEM were hydrated for 6 h before gold sputtering. C3A/gypsum samples for XRD analysis were hydrated for 1, 3, and 24 h.

Ettringite Synthesis. Samples of pure ettringite were prepared by modification of the previously described synthesis.[1] $Ca(OH)_2$ (1.59 g, 21.4 mmol) was dissolved in water (1.2 L) and mixed with a solution of $CaSO_4{\cdot}2H_2O$ (1.374 g, 8 mmol) in water (530 mL) for 1 h, at which point a solution of $Al_2(SO_4)_3{\cdot}18H_2O$ (1.78 g, 2.7 mmol) in water (770 mL) was added. The resulting aqueous solution was stirred for 2 h and then allowed to settle for 1 week. The resulting crystalline precipitate was collected by filtration. The formation of ettringite was confirmed by XRD [JCPDS # 41-1451].

Hydration in the Presence of H_6ntmp. The as-received solution of H_6ntmp (10 g of a 50 wt % solution) was diluted to 100-mL total solution volume to approximate a 5 wt % stock solution. Separate solid samples of CaO, $Ca(OH)_2$, and boehmite, [Al(O)(OH)], were hydrated with H_6ntmp solutions (0.5 mL of the 5 wt % H_6ntmp solution per 1.0 g of solid) for ^{31}P MAS NMR analysis. Gypsum ($CaSO_4{\cdot}2H_2O$) was hydrated with H_6ntmp (2 mL of the 5 wt % H_6ntmp solution per 1.0 g of solid) for ^{31}P MAS NMR analysis. H_6ntmp (0.6 g of the 50 wt % Aldrich solution, 0.1 mmol of H_6ntmp) was added to a solution of aluminum nitrate (0.67 g, 0.1 mmol) and in water (100 mL), resulting in a pH of about 3. A precipitate immediately formed and was analyzed by ^{31}P MAS NMR.

All C3A, C3S, and cement samples for NMR analyses were hydrated by the method described above using the 5 wt % stock solution of H_6ntmp (0.3 mL per 1.0 g of solid) in place of deionized water to create mineral pastes containing 1.5 wt % H_6ntmp unless otherwise noted. Cement samples were hydrated by three different methods for ^{31}P MAS NMR analysis. Cement was hydrated with a solution of H_6ntmp (0.5 mL per 1.0 g of cement of a 2 wt % H_6ntmp solution) to yield a paste containing 1 wt % H_6ntmp relative to the weight of dry cement. A second sample of cement was hydrated with water (0.3 mL per 1.0 g of cement) for 2 min, at which point a solution of H_6ntmp (0.2 mL of a 5 wt % H_6ntmp solution) was mixed into the paste and allowed to react for 10 min before NMR analysis. The third cement sample was hydrated with a more dilute solution of H_6ntmp (0.5 mL per 1.0 g of cement of a 0.6 wt % H_6ntmp solution) to yield a cement paste containing 0.3 wt % H_6ntmp relative to the weight of dry cement.

C3A samples for XPS analysis were hydrated with the 5 wt % H_6ntmp solution (0.5 mL per 1.0 g of solid) in a N_2 bag for 4.5 h, washed with acetone, and filtered. C3S samples for XPS analysis were hydrated with the 5 wt % H_6ntmp solution (0.5 mL per 1.0 g of solid) in a N_2 bag for either 7 h and then washed with acetone and filtered or hydrated for 1 week and analyzed without rigorous drying. Cement clinker samples for XPS were similarly hydrated for 7 h, washed with acetone, and filtered. Samples for SEM were hydrated using the stock 5 wt % H_6ntmp solution (0.3 mL per 1.0 g of solid) and allowed

(10) Bishop, M. Thesis, Rice University, 2001.

(11) *Annual Reports on NMR Spectroscopy*; Academic Press: New York, 1986; Vol. 28.

to hydrate for the following times: C3A, 4 h; C3A and gypsum samples (0.6 and 0.4 g, respectively), 6 h; C3S, 24 h and 1 week; C4AF, 6.5 h; cement, 7 h. Samples for liquid ^{31}P NMR were prepared by hydrating minerals with dilute solutions of H_6ntmp.

Synthesis of [Ca(H_4ntmp)(H_2O)]$_\infty$·3.5(H_2O)]. To an aqueous suspension of calcium hydroxide (0.74 g, 10 mmol, in 1 L) was added H_6ntmp (6.0 g of a 50% H_6ntmp mixture, ca. 10 mmol) until the solution cleared. The solution was boiled down (to ca. 100 mL) and allowed to cool to room temperature, producing a crystalline precipitate of colorless blocks suitable for single-crystal X-ray diffraction. This experiment was repeated using 2 equiv of calcium hydroxide (0.74 g, 10 mmol, in 1 L) to H_6ntmp (3 g of the 50% H_6ntmp mixture, ca. 5 mmol). The solution never fully cleared. The insoluble material formed was analyzed by ^{31}P MAS NMR. The solution filtrate was boiled down (to ca. 50 mL) and cooled to room temperature. Unit cell measurements confirmed the sample to be [Ca(H_4ntmp)(H_2O)]$_\infty$·3.5(H_2O)]. mp: 118 °C (dec). DRIFT IR (cm^{-1}): 1642 (s br), 1433 (s), 1314 (w), 1164 (s br), 1073 (s br), 1023 (s), 937 (s), 805 (w), 550 (m). ^{13}C CPMAS NMR: δ 55.4 (CH_2), 53.7 (CH_2), 51.0 (CH_2). ^{31}P CPMAS NMR: δ 11.7 (1P), 4.41 (2P).

Crystallographic Studies. Data for compounds [Ca(H_4ntmp)(H_2O)]$_\infty$·3.5(H_2O)] was collected on a Bruker CCD SMART system, equipped with graphite monochromated Mo Kα radiation (λ = 0.71073 Å) and corrected for Lorentz and polarization effects. The structure was solved using the direct methods program XS[12] and difference Fourier maps and refined by using full-matrix least-squares methods. All non-hydrogen atoms were refined with anisotropic thermal parameters. Hydrogen atoms were introduced in calculated positions and allowed to ride on the attached carbon atoms [d(C−H) = 0.95 Å]. Refinement of positional and anisotropic thermal parameters led to convergence. [Ca(H_4ntmp)(H_2O)]$_\infty$·3.5(H_2O)]: $C_3H_{19}CaNO_{13.5}P_3$, M = 417.75, monoclinic, a = 11.252(2) Å, b = 8.475(2) Å, c = 15.633(3) Å, β = 90.25(3)°, U = 1490.8(5) Å^3, space group $P2_1/n$ (No. 14), Z = 4, 6715 reflections measured, 2166 unique of which 1452 [$F > 4\sigma(F)$] were used in all calculations. The final R was 0.0464 and R_w 0.1086, weighting scheme (SHELXTL parameters) 00401, 0.

Results and Discussion

Reaction of H_6ntmp with Calcium Salts. Polyphosphates can enhance the solubility of calcium hydroxide in water, both because they reduce the pH of the solution and are capable of chelating Ca^{2+}.[5] In the case of H_6ntmp (**I**) the enhanced solubility is temporary. Addition of H_6ntmp to an aqueous suspension of Ca($OH)_2$ initially results in a clear solution; however, a white solid precipitates over time.

The soluble [Ca($H_n$ntmp)]$^{(4-n)-}$ species was observed with ^{31}P NMR spectroscopy using dilute solutions of Ca($OH)_2$ and an equimolar or slight excess of H_6ntmp. With excess H_6ntmp the solution ^{31}P NMR spectrum shows a triplet at δ = 9.0 ppm [J(P−H) = 12 Hz] while under equimolar conditions a broad singlet (δ = 9.8 ppm) is observed. The transition between these spectra is as a consequence of the slight increased acidity (pH 6 versus pH 7) for solutions with an excess of H_6ntmp and the deprotonation of the [Ca($H_n$ntmp)]$^{(4-n)-}$ species.

The rate of precipitation varies with the concentrations of both Ca^{2+} and H_6ntmp, and the solution pH. If dilute solutions are employed, a small quantity of colorless crystals is initially formed. In contrast, use of more concentrated solutions leads to rapid precipitation of a polycrystalline powder that is chemically and

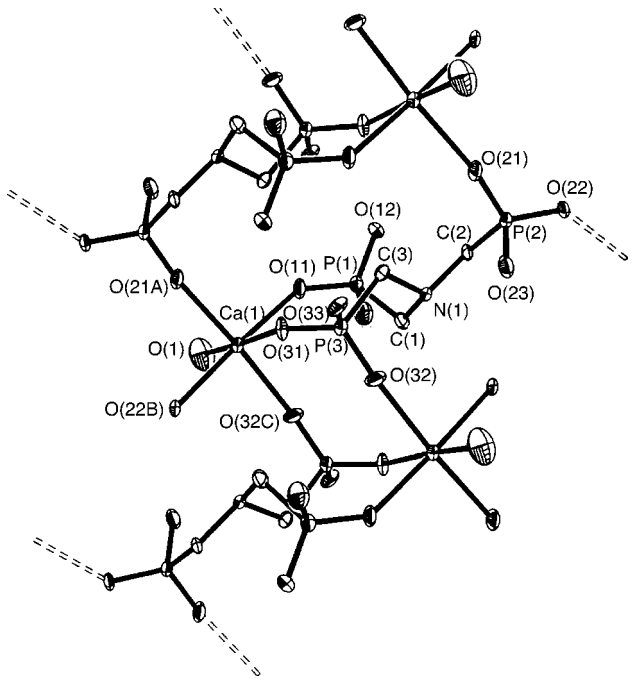

Figure 2. View of the sheet structure of [Ca(H_4ntmp)(H_2O)]$_\infty$. Thermal ellipsoids are shown at the 50% level. All hydrogen atoms and water of crystallization are omitted for clarity. P(2) and P(3) bridge two calcium atoms, and P(1) is associated with only a single calcium atom.

structurally identical to the single crystals (see below). From single-crystal X-ray diffraction measurements the structure of this crystalline material was determined to be [Ca(H_4ntmp)(H_2O)]$_\infty$·3.5(H_2O) (Figures 2−4); selected bond lengths and angles are given in Table 1.

The calcium atoms in [Ca(H_4ntmp)(H_2O)]$_\infty$ have octahedral coordination through five phosphonate interactions and a coordinated water [O(1)]. All the Ca−O distances are within the range previously reported for phosphonate compounds [2.305(2)−2.511(1) Å].[13−16] There are two types of phosphonate moiety: one terminal [P(1)] (**II**) and two bridging [P(2) and P(3)] (**III**).

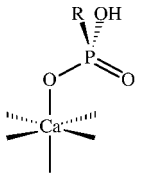

(**II**)

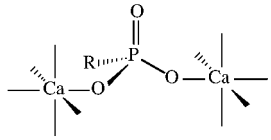

(**III**)

The P−O distances in uncomplexed [H_4ntmp]$^{2-}$ were reported to be divided into three groups: the shortest (average 1.477 Å) associated with P═O bonds, the longest (average 1.534 Å) associated with P−OH bonds, and the intermediate (average 1.501 Å) described at P−O$^-$ bonds in which the oxygen carries a negative charge.[17] Similarly, in [Ca(H_4ntmp)(H_2O)]$_\infty$, the P−OH bonds are the longest [1.560(4)−1.569(4) Å]. However,

(12) Sheldrick, G. M. *SHELXTL*; Bruker AXS, Inc.: Madison, WI, 1997.

(13) Langley, K. J.; Squattrito, P. J.; Adani, F.; Montoneri, E. *Inorg. Chim. Acta* **1996**, *253*, 77.

(14) Rudolf, P. R.; Clarke, E. T.; Martell, A. E.; Clearfield, A. *Acta Crystallogr.* **1988**, *C44*, 796.

(15) Smith, P. H.; Raymond, K. N. *Inorg. Chem.* **1988**, *27*, 1056.

(16) Cao, G.; Lynch, V. M.; Swinnea, J. S.; Mallouk, T. E. *Inorg. Chem.* **1990**, *29*, 2112.

(17) Daly, J. J.; Wheatly, P. J. *J. Chem. Soc. A* **1967**, 212.

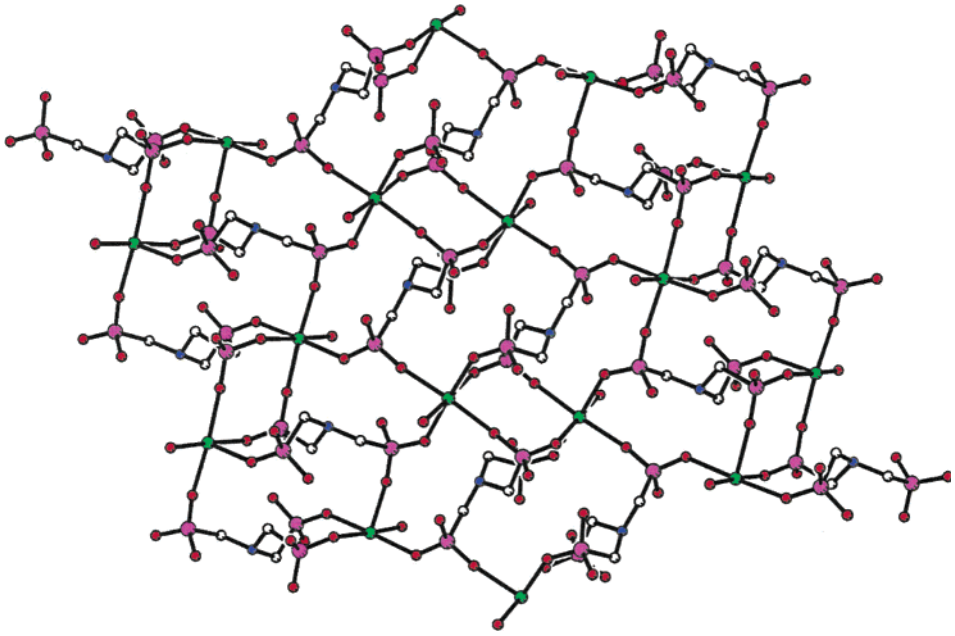

Figure 3. A planar sheet of $[Ca(H_4ntmp)(H_2O)]_\infty$. Atom color scheme: calcium (green), oxygen (red), phosphorus (purple), and nitrogen (blue).

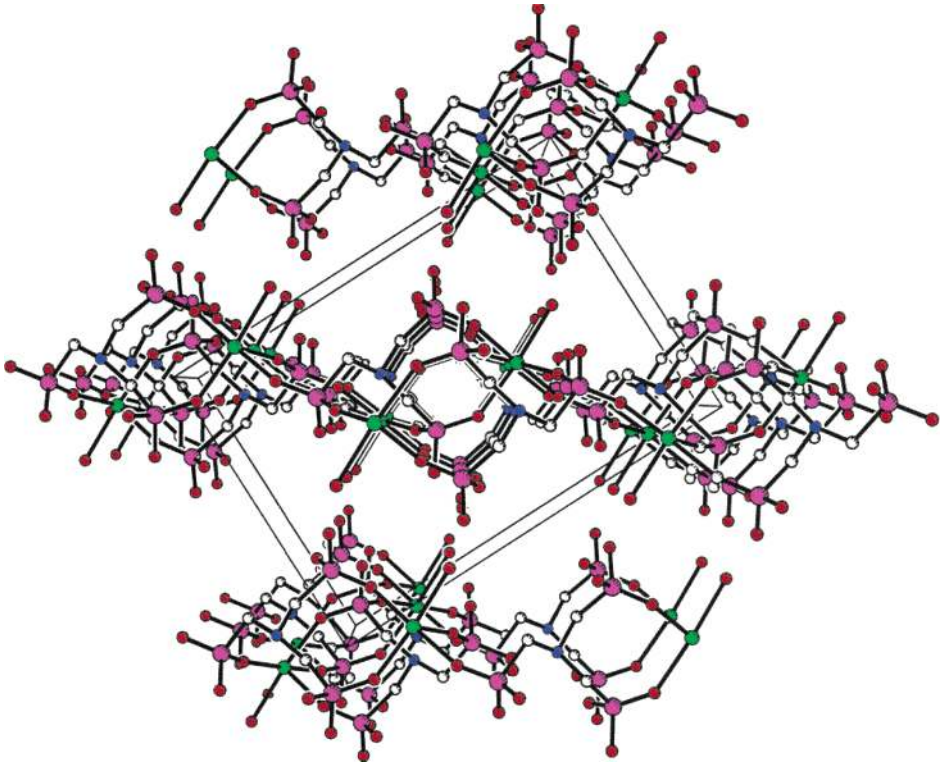

Figure 4. Crystal packing of $[Ca(H_4ntmp)(H_2O)]_\infty$ viewed along the *b*-axis. All hydrogen atoms and water of crystallization are omitted for clarity. Atom color scheme: calcium (green), oxygen (red), phosphorus (purple), and nitrogen (blue).

the uncomplexed P═O bond length [1.488(4) Å] appears in the range of bond lengths found for the P−O/P═O bonds associated with calcium [1.474(4)−1.503(3) Å]. On the basis of the charge balance and the relative P−O distances, one oxygen per phosphonate group is protonated along with the amine's nitrogen.[15,18] The Ca−O−P angles are grouped into two ranges: 135.1(2)−142.9(2)° and 169.6(2)−170.1(2)°. Although there is no clear correlation between the Ca−O−P angle and either the Ca−O or P−O bond distances, there is a good correlation between the Ca−O and P−O bond distances; see Figure 5.

The structure of $[Ca(H_4ntmp)(H_2O)]_\infty$ may be described as adopting hierarchical level of crystal architecture consisting of two types of dimer (*primary* level, Figure 2) interactions, creating a series of planar sheets (*secondary* level, Figure 3) which are coplanar and contain intersheet contacts via hydrogen-bonded waters of crystallization (*tertiary* level, Figure 4). It is this infinite sheetlike structure that is important with

(18) (a) Motekaitis, R.; Martell, A. *J. Coord. Chem.* **1985**, *14*, 139. (b) Sprankle, P.; Meggitt, W.; Penner, D. *Weed Sci.* **1975**, *76*, 1304.

Table 1. Selected Bond Lengths (Å) and Angles (deg) for $[Ca(H_4ntmp)(H_2O)]_\infty$[a]

Ca(1)−O(11)	2.296(3)	Ca(1)−O(21A)	2.266(4)
Ca(1)−O(31)	2.344(4)	Ca(1)−O(22B)	2.324(3)
Ca(1)−O(32C)	2.288(3)	Ca(1)−O(1)	2.386(4)
P(1)−O(11)	1.483(3)	P(1)−O(12)	1.488(4)
P(1)−O(13)	1.569(4)	P(2)−O(21)	1.474(4)
P(2)−O(22)	1.487(3)	P(2)−O(23)	1.560(4)
P(3)−O(31)	1.503(3)	P(3)−O(32)	1.483(4)
P(3)−O(33)	1.565(4)		
O(11)−Ca(1)−O(22C)	176.3(1)	O(21A)−Ca(1)−C(32B)	175.6(1)
O(31)−Ca(2)−O(1)	174.3(1)	Ca(1)−O(11)−P(1)	142.9(2)
Ca(1A)−O(21)−P(2)	169.6(2)	Ca(1D)−O(22)−P(2)	135.1(2)
Ca(1)−O(31)−P(3)	142.4(2)	Ca(1B)−O(32)−P(3)	170.1(2)

[a] Symmetry transformations used to generate equivalent atoms: A $(1-x, 1-y, 1-z)$, B $(1-x, -y, 1-z)$, C $(x+{}^1/_2, {}^1/_2-y, z-{}^1/_2)$, D $(x-{}^1/_2, {}^1/_2-y, z-{}^1/_2)$.

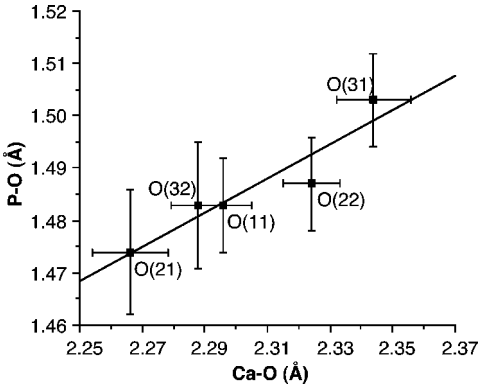

Figure 5. Plot of P−O bond (Å) versus Ca−O bond length (Å) in $[Ca(H_4ntmp)(H_2O)]_\infty$.

regard to the function of H_6ntmp as a cement inhibitor; see below.

Of the two types of dimer interactions shown in Figure 2, the first may be considered to consist of two calcium atoms bridged by two phosphonate groups forming an eight-membered ring analogous to those observed for group 13 phosphonates[19] and phosphinates,[20] as well as carboxylates, amides, phosphoramides, and triflates.[21] Of the remaining phosphonate groups on each $[H_4ntmp]^{2-}$ ligand, one chelates a calcium in the dimer [via O(11)] and the other bridges two adjacent dimeric units [via O(21) and O(22)]. The second dimeric subunit consists of a H_4ntmp ligand chelating one calcium atom [via O(11) and O(31)] and bridges two other calciums [via O(23) and O(22)]. The $[H_4ntmp]^{2-}$ ligand chelates in a wrap-around fashion using two phosphonate termini, not through a four-membered chelate ring associated with one phosphonate moiety. This is in contrast to the structure reported for $[Ca(O_3PCH_2NH_2CH_2CO_2)]_\infty(H_2O)_2$.[15,18]

As noted above, the solid-state structure was determined from a single crystal obtained under slow precipitation conditions. To confirm that the structure of $[Ca(H_4ntmp)(H_2O)]_\infty$ is representative of the calcium-containing product obtained from the reaction under a variety of other concentration conditions, the X-ray

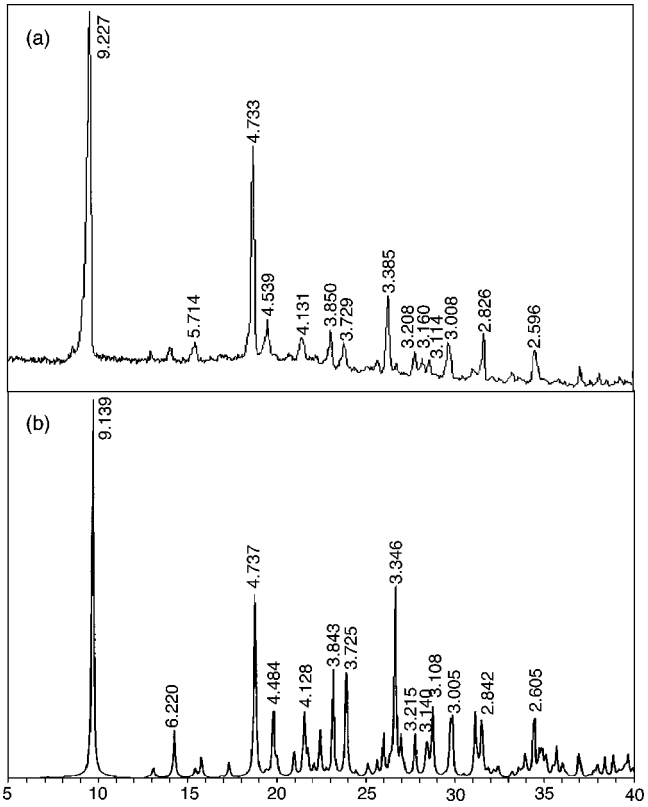

Figure 6. X-ray powder diffraction of (a) polycrystalline precipitate from the reaction of $Ca(OH)_2$ and H_6ntmp and (b) the computer-simulated powder diffraction (XPOW) from the single-crystal structure solution of $[Ca(H_4ntmp)(H_2O)]_\infty \cdot 3.5(H_2O)$.

powder pattern for a series of samples was compared with the powder pattern calculated from the single-crystal data solution. The X-ray powder diffraction pattern (Figure 6a) of a polycrystalline powder obtained from the reaction of $Ca(OH)_2$ with H_6ntmp clearly matches (*d*-spacing and relative intensity) the theoretical powder pattern generated using XPOW[12] from the single-crystal structure solution (Figure 6b). Thus, all the crystalline products are of the same material, albeit with possible variations in water of crystallization.

Samples of $[Ca(H_4ntmp)(H_2O)]_\infty$ yield a ^{31}P MAS NMR spectrum with two peaks, at $\delta = 11.7$ and 4.4 ppm (Figure 7a) due to the terminal (**II**) and bridging (**III**) phosphonate moieties, respectively. A crystalline sample of $[Ca(H_4ntmp)(H_2O)]_\infty$ was exposed to concentrated NaOH and $Ca(OH)_2$ to determine the effect on the structure of excess base and calcium, respectively. The ^{31}P MAS NMR spectrum of $[Ca(H_4ntmp)(H_2O)]_\infty$ exposed to a concentrated NaOH solution for 12 h reveals that the proportion of terminal phosphonate groups ($\delta = 11.7$ ppm, **II**) has increased with respect to the bridging phosphonate groups ($\delta = 4.4$ ppm, **III**); see Figure 7b. Therefore, the OH^- ions compete favorably for calcium in basic solutions and disrupt some of the bridging phosphonate interactions. In contrast, after exposure of the crystals to $Ca(OH)_2$ for 12 h, more bridging moieties ($\delta = 4.4$ ppm, **III**) are observed relative to the number of terminal phosphonates ($\delta = 11.7$ ppm, **II**) and an additional peak near 20 ppm is present (Figure 7c). The peak at $\delta = 20$ ppm is due to the $[Ca_3(ntmp)]$ complex, based on a comparison to previous solution ^{31}P NMR data which revealed $[Ca(ntmp)]^{4-}$ at $\delta = 18$ ppm. In the

(19) Mason, M. R. *J. Cluster Sci.* **1998**, *9*, 1 and references therein.
(20) (a) Hahn, F. E.; Schneider, B. *Z. Naturforsch. B* **1990**, *45*, 134. (b) Landry, C. C.; Hynes, A.; Barron, A. R.; Haiduc, I.; Silvestru, C. *Polyhedron* **1996**, *15*, 391.
(21) (a) Keys, A.; Bott, S. G.; Barron, A. R. *Polyhedron* **1998**, *17*, 3121. (b) Keys, A.; Barbarich, T.; Bott, S. G.; Barron, A. R. *J. Chem. Soc., Dalton Trans.* **2000**, 577.

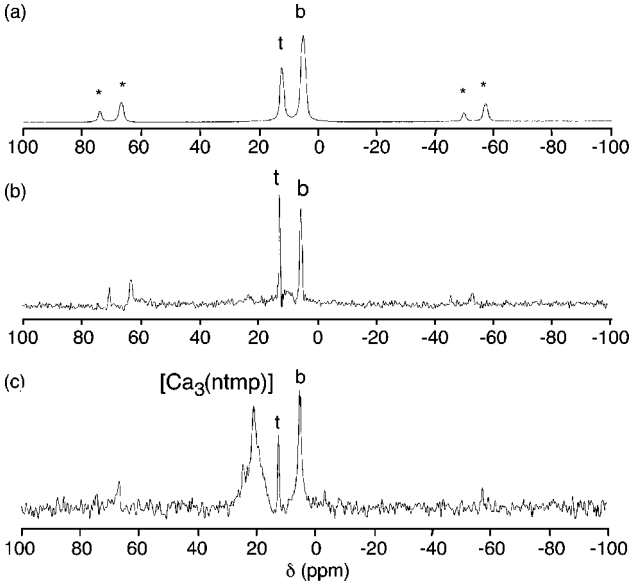

Figure 7. ^{31}P MAS NMR spectra of (a) $[Ca(H_4ntmp)(H_2O)]_\infty \cdot 3.5(H_2O)$ showing a 2:1 ratio of bridging to terminal phosphonates, (b) $[Ca(H_4ntmp)(H_2O)]_\infty \cdot 3.5(H_2O)$ exposed to NaOH, and (c) $[Ca(H_4ntmp)(H_2O)]_\infty \cdot 3.5(H_2O)$ exposed to $Ca(OH)_2$. Spinning sidebands are marked (*).

solid state, the fully deprotonated ligand must be associated with more calcium ions to balance the negative charge. Sawada et al. reported that the fully monoprotonated ligand (with the proton on the nitrogen) bound to calcium in a *fac*-chelate fashion in which all of the phosphonate−calcium interactions are terminal.[22]

In oil field applications, cement is hydrated with a limited amount of water. The amount of water used is reported as weight of water per weight of solid (w/s), with values of 0.3−0.7 w/s being used, depending on the applications. To provide a comparison of the speciation close to actual "in-field" conditions, it is necessary to characterize the reaction of H_6ntmp with calcium oxide and hydroxide under similar conditions. The ^{31}P MAS NMR of $[Ca(H_4ntmp)(H_2O)]_\infty$ was used to interpret the spectra of H_6ntmp reacted with CaO, $Ca(OH)_2$, and $CaSO_4 \cdot 2(H_2O)$ (gypsum) with a limited amount of water present. Samples were prepared by wetting calcium oxide and calcium hydroxide with H_6ntmp (5 wt %) to create pastes with the consistency of freshly hydrated cement. The ^{31}P MAS NMR spectra for both samples revealed peaks at $\delta = 19$ and 3 ppm. These peaks are all very broad, suggesting that the phosphonates exist in a multitude of different environments possibly due to poor crystallinity. The peak at $\delta = 19$ ppm is due to a fully deprotonated phosphonate coordinated to calcium, while the peak at ca. 3 ppm is most likely due to a bridging moiety (i.e., **III**). Hydration of gypsum, $CaSO_4.2(H_2O)$, in the presence of H_6ntmp results in the formation of $[Ca(H_4ntmp)]$ ($\delta = 11.6$ and 4.4 ppm).

Reaction of H_6ntmp with Tricalcium Silicate. The tri- and dicalcium silicates (C3S and C2S, respectively) comprise over 80 wt % of most Portland Cements. It is known that C3S is the most important phase in cement for strength development during the first month, while C2S reacts much more slowly, and contributes to the long-term strength of the cement.[1] Both the silicate phases react with water as shown below to form calcium hydroxide and a calcium−silicon−hydrate rigid gel, C−S−H (eqs 1 and 2).[23,24]

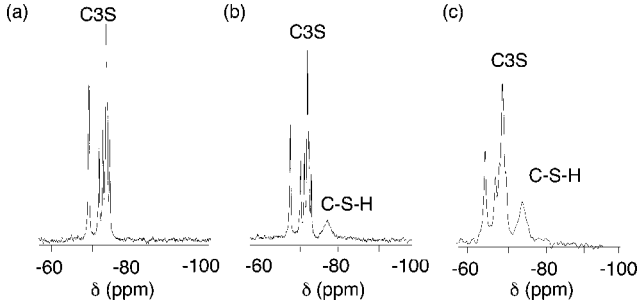

Figure 8. ^{29}Si MAS NMR of (a) anhydrous C3S, (b) C3S after 22 h of hydration, and (c) C3S after 42 h of hydration.

$$2(CaO)_3(SiO_2) + 7H_2O \rightarrow (CaO)_3(SiO_2)_2 \cdot 4(H_2O) + 3Ca(OH)_2 \quad (1)$$

$$2(CaO)_2(SiO_2) + 5H_2O \rightarrow (CaO)_3(SiO_2)_2 \cdot 4(H_2O) + Ca(OH)_2 \quad (2)$$

The ^{29}Si MAS NMR spectrum of anhydrous C3S shows five peaks in the range normally associated with SiO_4 species (Figure 8a). Hydration of C3S and subsequent formation of C−S−H is readily observed by ^{29}Si MAS NMR.[25] During hydration, the anhydrous silicate species give way to the hydrated dimers and higher polysilicate chain species found in C−S−H (Figure 8b,c). The evolution of the dimeric silicate chains is marked by the growth of the broad peak at $\delta = -78$ ppm.

The C−S−H gel also has a unique morphology that can be easily observed by SEM. The anhydrous grains appear smooth and are typically a few micrometers wide in size (Figure 9a). After hydration, tapered rods of

(22) Sawada, K.; Kanada, T.; Naganuma, Y.; Suzuki, T. *J. Chem. Soc., Dalton Trans*. **1993**, 2557.

(23) The detailed structure of C−S−H is not completely known; however, it is generally agreed upon that it consists of condensed silicate tetrahedra sharing oxygen atoms with central, calcium hydroxide-like CaO_2 layers (consisting of hexagonal layers of octahedrally coordinated calcium atoms and tetrahedrally coordinated oxygen atoms). It is proposed that the structure is most similar to either Tobermorite or Jennite, both of which share a skeletal silicate chain structure, Taylor, H. F. W. *J. Am. Ceram. Soc.* **1986**, *69*, 464.

(24) The hydration of the calcium silicates proceeds via four distinct phases. The first 15−20 min, termed the pre-induction period, is marked by rapid heat evolution. During this period calcium and hydroxyl ions are released into the solution. The next phase is the induction period, during which time calcium oxide continues to dissolve, producing a pH near 12.5. It has been suggested that, in pure C3S, the induction period may be the length of time it takes for C−S−H to begin nucleation. Alternatively, the induction period may be caused by the development of a small amount of an impermeable calcium−silicon−hydrate (C−S−H) gel at the surface of the particles, which slows down the migration of water to the inorganic oxides. As the initial C−S−H gel is transformed into the more permeable layer, hydration continues and the induction period gives way to the third phase of hydration, the acceleratory period. Hardening (setting) occurs near the end of the third period. The fourth stage is the deceleratory period in which hydration slowly continues until the reaction is complete. The rate of hydration in the deceleratory period is determined either by the slow migration of water through C−S−H to the inner, unhydrated regions of the particles, or by the migration of H^+ through the C−S−H to the anhydrous CaO and SiO_2, and the migration of Ca^{2+} and Si^{4+} to the OH^- ions left in solution. (a) Ramanchandran, V. S.; Feldman, R. F.; Beaudoin, J. J. *Concrete Science*; Heyden and Son Ltd.: Philadelphia, PA, 1981. (b) Stein, H. N.; Stevels, J. *J. Appl. Chem.* **1964**, *14*, 338. (c) Grutzeck, M.; Kwan, S.; Thompson, J.; Benesi, A. *J. Mater. Sci. Lett.* **1999**, *18*, 217.

(25) Barnes, J. R.; Clague, A. D. H.; Clayden, N. J.; Dobson, C. M.; Hayes, C. J.; Groves, G. W.; Rodger, S. A. *J. Mater. Sci. Lett.* **1985**, *4*, 1293.

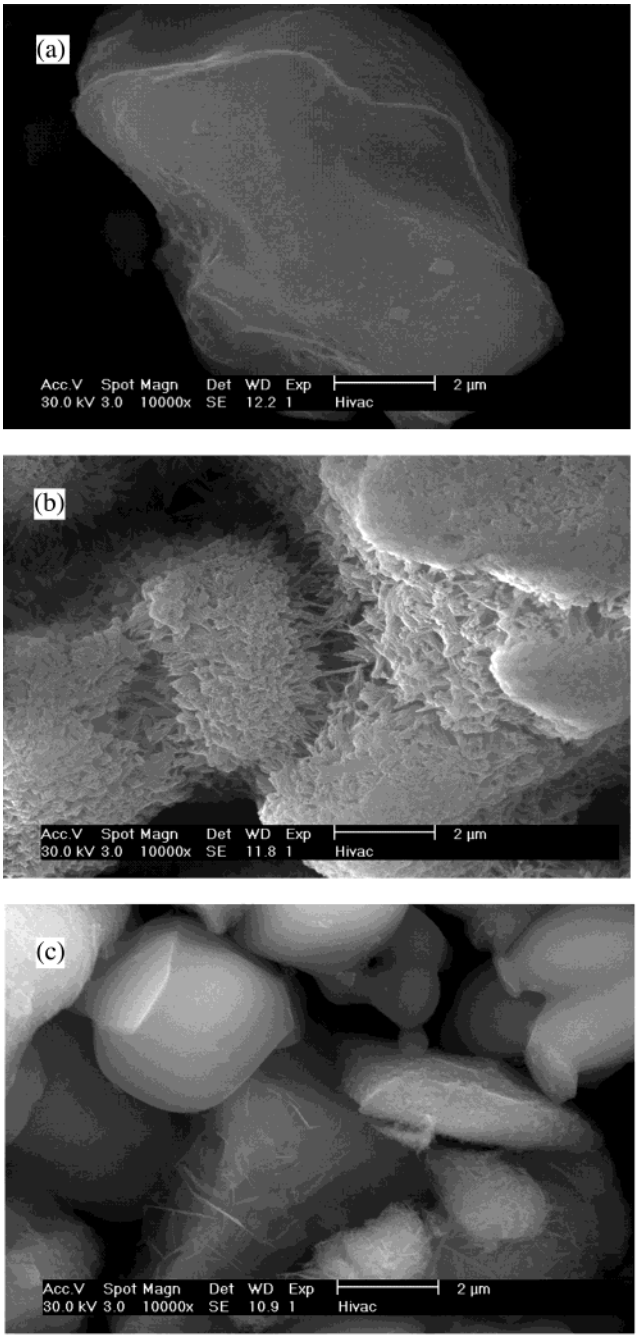

Figure 9. SEM images of (a) anhydrous C3S, (b) C3S after 2 weeks of hydration, and (c) C3S after 24 h of hydration in the presence of H_6ntmp (1.5 wt %).

C−S−H grow from the C3S grains.[26] Over time, these needles become more interlocked and take on a foil-like morphology and eventually C−S−H connects adjacent particles (Figure 9b).

The hydration of C3S in the presence of H_6ntmp (1.5 wt %) was followed by SEM, NMR, and XPS. SEM images of C3S hydrated for 24 h in the presence of H_6ntmp (Figure 9c) do not appear appreciatively different from an nonhydrated sample (Figure 9a). The lack of hydration is confirmed by ^{29}Si NMR spectroscopy, which reveals that in the presence of H_6ntmp no dimeric silicate species (i.e., no peak at −78 ppm) are formed, even after 2 weeks of hydration. This should be compared to the spectrum of C3S hydrated without retarders, in which a significant amount of C−S−H forms after just 1 day of hydration (Figure 8b).

XPS analysis was performed on C3S samples, with and without H_6ntmp (1.5 wt %), hydrated for 7 h and 1 week for both samples. The Ca:Si ratio for a sample of C3S changes from 2.6 to 2.4 during that time, consistent with the formation of C−S−H (eq 1). The Ca:Si ratio in the sample hydrated in the presence of H_6ntmp is initially low (1.8); however, it reached a value of 3.0 after 1 week of hydration. The low initial Ca:Si ratio could be consistent with either a calcium complexation or nucleation poisoning mechanism; however, the high final Ca:Si ratio does not fit either model. The increase in the Ca:Si ratio is consistent with the precipitation of a calcium-rich phase such as the phosphonate complex. The ^{31}P MAS NMR spectra of C3S hydrated with a limited amount of water (0.3 w/s) and H_6ntmp (0.75 wt %) reveals a large peak at 19 ppm, due to [Ca_3(ntmp)], and several smaller peaks spanning the region from 10 to 1 ppm associated with both terminal (**II**) and bridging (**III**) phosphonates.

Reaction of H_6ntmp with Tricalcium Aluminate. Although the aluminate and ferrite phases comprise less than 20% of the bulk of cement, their reactions are very important in cement and dramatically affect the hydration of the calcium silicate phases. Relative to C3S, the hydration of C3A [$(CaO)_3(Al_2O_3)$] is very fast. In the absence of any additives, C3A reacts with water to form two intermediate hexagonal phases, C2AH8 and C4AH13 (eq 3).[27] C2AH8 and C4AH13 are metastable phases that spontaneously transform into the fully hydrated, thermodynamically stable cubic phase, C3AH6 (eq 4).

$$2(CaO)_3(Al_2O_3) + 21H_2O \rightarrow (CaO)_4(Al_2O_3)\cdot 13(H_2O) + (CaO)_2(Al_2O_3)\cdot 8(H_2O) \quad (3)$$

$$(CaO)_4(Al_2O_3)\cdot 13(H_2O) + (CaO)_2(Al_2O_3)\cdot 8(H_2O) \rightarrow 2(CaO)_3(Al_2O_3)\cdot 6(H_2O) + 9(H_2O) \quad (4)$$

The aluminum coordination in C3A is distorted tetrahedral, whereas the aluminum in C3AH6 exists in highly symmetrical, octahedral $[Al(OH)6]^{3-}$ units allowing for hydration to be conveniently followed by ^{27}Al NMR spectroscopy. Although aluminum is spin $^5/_2$ and in general exhibits a large quadrupolar coupling constant, several distinct species can be observed during hydration.[28] The chemical shifts of the hexagonal phases, C2AH8 and C4AH13, lie within 10 ppm of C3AH6 and the lines due to all of these phases are broader than 10 ppm at both 52.1 and 130.3 MHz; however, the transition from the hexagonal phases to the cubic phase can be observed as an upfield shift even on a 200-MHz (^{27}Al

(26) The C−S−H takes on a more spiked, needlelike appearance as it becomes partially dehydrated under the high-vacuum conditions necessary for SEM imaging.

(27) The structure of C2AH8 is not precisely known, but structures containing $[Ca_2Al(OH)_6][Al(OH)_4]\cdot nH_2O$ or $[Ca_2Al(OH)_6][Al(OH)_3(H_2O)_3]$-OH have been proposed. C4AH13 has a layered structure based on the calcium hydroxide structure in which one out of every three Ca^{2+} is replaced by an Al^{3+} or Fe^{3+} with an OH^- anion in the interlayer space to balance the charge. All of the aluminum centers in C4AH13 are octahedral.

(28) (a) Skibsted, J.; Hendricson, E.; Jakobsen, H. J. *Inorg. Chem.* **1993**, *32*, 1013. (b) Faucon, P.; Charpentier, T.; Bertrandie, D.; Nonat, A.; Virlet, J.; Petit, J. C. *Inorg. Chem.* **1998**, *37*, 3726.

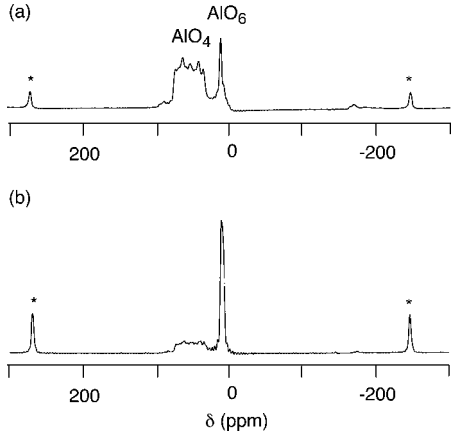

Figure 10. ^{27}Al MAS NMR at 130.3187 MHz of C3A (a) and (b) after 30 min hydration. Spinning sidebands are marked (*).

observed frequency 52.1476 MHz) spectrometer. The highly distorted anhydrous tetrahedral aluminum is difficult to observe on a 200-MHz instrument, but is readily observed at 500 MHz (observed frequency 130.3187 MHz). At 52 MHz, the tetrahedral phase is not observed; however, the growth of the intermediate hexagonal phases C2AH8 and C4AH13 shown by the signal near $\delta = 8$ ppm and the subsequent downfield shift of this peak to $\delta = 11$ ppm to indicate C3AH6 formation is readily apparent. In contrast, at 130 MHz (Figure 10) the transition from a tetrahedral phase ($\delta = 40-80$ ppm) to an octahedral phase ($\delta = 8$ ppm) and then a downfield shift to the highly symmetrical C3AH6 species is clearly observed.

The hydration of C3A in the presence of H_6ntmp (1.5 wt %) was monitored using ^{27}Al MAS spectroscopy. On a 200-MHz spectrometer, no tetrahedral aluminum is observed. The octahedral species appears at 6 ppm, slightly upfield of the normal shift expected for the partially hydrated, hexagonal calcium aluminate intermediates. This peak continues to grow in for the first hour and then shifts slightly to $\delta = 7.8$ ppm after 2 h, suggesting the formation of C2AH8 and C4AH13 (cf., Figure 10b). After 3 days of hydration the spectrum shows a slight increase in signal intensity, but no C3AH6 is observed. This is in contrast to the spectra observed for C3A hydration in the absence of additives, which shows significant C3AH6 formation after just 30 min.

C3A hydration with H_6ntmp (1.5 wt %) was investigated by ^{31}P MAS NMR spectroscopy. Peaks at $\delta = 18.4$ and 3.4 ppm were observed, a spectrum most similar to that observed for calcium hydroxide hydrated with 1.5% H_6ntmp. No peaks due to aluminum phosphonate complexes were observed,[10] indicating that under these conditions, reaction with calcium is favored over aluminum.

The hydration of C3A in the presence of H_6ntmp (1.5 wt %) was also followed by SEM. After 4 h, the development of a foil-type layer on the C3A particles is observed, similar to that observed for the hydration of pure C3A but with much smaller features. XPS analysis of C3A hydrated for 4 h in the presence of H_6ntmp (2.5 wt %) reveals a P:Ca ratio is 1.6 (i.e., ca. 2 Ca per molecule of H_6ntmp). In addition, there is a change in the Ca:Al ratio from 0.9:1 in the anhydrous mineral to

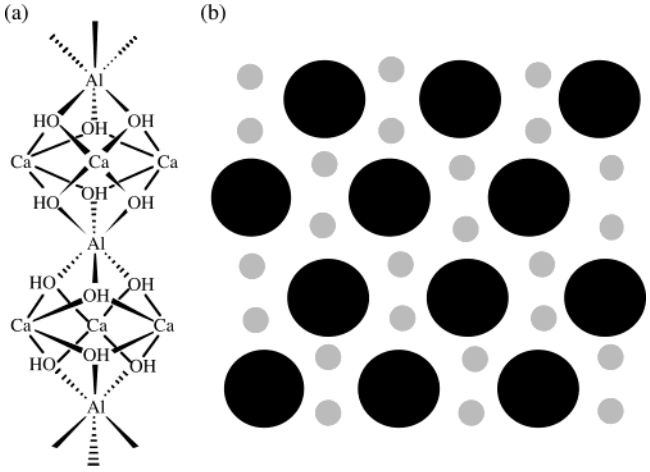

Figure 11. Ettringite columns (a) consisting of octahedral aluminum, tetrahedral oxygen, and 8-coordinate calcium. The coordination sphere of each calcium is completed by water and sulfate ions. The packing of the columns (b) represented by large circles; the smaller circles represent channels containing water and sulfate ions.

11.6:1. This should be compared to the Ca:Al ratio of 1.7:1 observed for the uninhibited paste. This result indicates that aluminum is buried under a Ca−P-rich layer.

Reaction of H_6ntmp with Tricalcium Aluminate in the Presence of Gypsum. If the very rapid and exothermic hydration of C3A is allowed to proceed unhindered in cement, then the setting occurs too quickly and the cement does not develop strength. Therefore, gypsum [calcium sulfate dihydrate, $CaSO_4 \cdot 2(H_2O)$] is added to slow the C3A hydration. In the presence of gypsum, tricalcium aluminate forms the needlelike mineral ettringite, $[(CaO)_3(Al_2O_3)(CaSO_4)_3 \cdot 32(H_2O)]$ (eq 5). The structure of ettringite consists of columns of calcium, aluminum, and oxygen surrounded by water and sulfate ions, as shown in Figure 11. If insufficient sulfate is present, then the ettringite will eventually react with excess C3A to form the monosulfate, $C3A \cdot CaSO_4 \cdot 12(H_2O)$ (eq 6). However, the reactions

$$(CaO)_3(Al_2O_3) + 3CaSO_4 \cdot 2(H_2O) + 26H_2O \rightarrow [(CaO)_3(Al_2O_3)(CaSO_4)_3 \cdot 32(H_2O)] \quad (5)$$

$$[(CaO)_3(Al_2O_3)(CaSO_4)_3 \cdot 32(H_2O)] + 2(CaO)_3(Al_2O_3) + 4H_2O \rightarrow 3(CaO)_3(Al_2O_3)(CaSO_4) \cdot 12(H_2O) \quad (6)$$

that affect hydration inhibition occur during the induction period, and the monosulfate forms after the end of the induction period. Thus, we have assumed that this last step in the hydration of C3A in the presence of gypsum is not important to the investigation into the mechanisms of hydration inhibition.

The ^{27}Al MAS of C3A hydrated in the presence of excess gypsum indicates that the ettringite formation proceeds via partially hydrated calcium aluminate species, possibly C2AH8 and C4AH13. The formation of ettringite may also be seen from the growth of crystalline rods from the surface of C3A (Figure 12). The rods generally range from 1 to 2 μm in length and are about 10−20-nm wide when grown in situ from pastes of C3A and gypsum. Phase conformation of ettringite is ob-

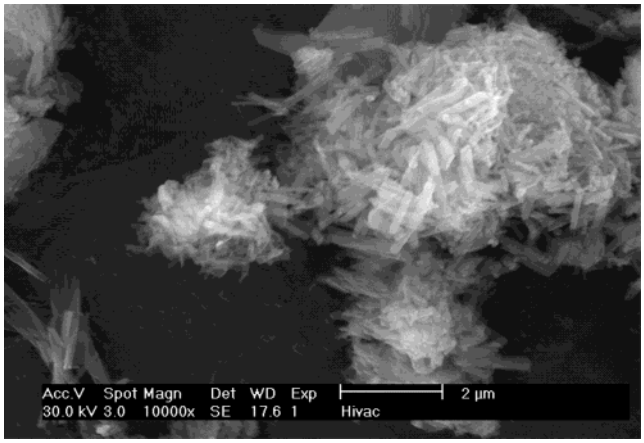

Figure 12. SEM image of C3A hydrated in the presence of gypsum showing the formation of ettringite.

tained from its low-angle powder X-ray tag ($d = 9.8$ Å) that allows it to be easily distinguished from residual calcium sulfate ($d = 7.7$ Å).

The effect of H_6ntmp on the hydration of C3A in the presence of gypsum was investigated using ^{27}Al and ^{31}P MAS NMR and XRD. The ^{31}P MAS NMR spectrum of C3A hydrated in the presence of excess gypsum with a dilute H_6ntmp solution is markedly different from the comparable spectrum without gypsum. In the presence of excess gypsum, there is a small peak at $\delta = 16$ ppm and a larger peak at $\delta = 6$ ppm with a second maximum near $\delta = 3$ ppm and a broad shoulder that extends out to -10 ppm, the latter feature suggesting that complexation to aluminum should not be ruled out.[29]

^{27}Al MAS NMR of C3A hydrated in the presence of gyspum and 1.5 wt % H_6ntmp reveals initial *accelerated* formation of ettringite, followed by a long period of slow reactivity.[30] Figure 13 compares the hydration of C3A with excess gypsum with and without the H_6ntmp solution (1.5 wt %) during the first 30 min of hydration. The 10-min spectrum of C3A with gypsum and H_6ntmp shows ettringite (centered at $\delta = 13$ ppm) and a partially hydrated calcium aluminate (C2AH8 and C4AH13, $\delta = 8$ ppm) present in about a 1:1 ratio (Figure 13a). This spectrum remains unchanged after 30 min. In contrast, the spectra in the absence of the retarder (Figure 13b) show the transition from the hydrated calcium aluminate intermediate ($\delta = 8$ ppm) to ettringite ($\delta = 13$ ppm). After 30 min, the spectrum taken in the absence of H_6ntmp shows almost complete conversion to ettringite, while the spectrum with H_6ntmp still shows a significant amount of partially hydrated calcium aluminates.

Reaction of H_6ntmp with Tricalcium Aluminoferrite. Tetracalcium aluminoferrite (C4AF) reacts much like C3A, i.e., with the formation of an iron-substituted ettringite in the presence of gypsum. However, hydration of the ferrite phase is much slower than that of C3A.[31] In addition, if in a cement there is insufficient gypsum to convert all of the C4AF to ettringite, then an iron-rich gel forms at the surface of the silicate particles, which is proposed to slow their hydration.[32]

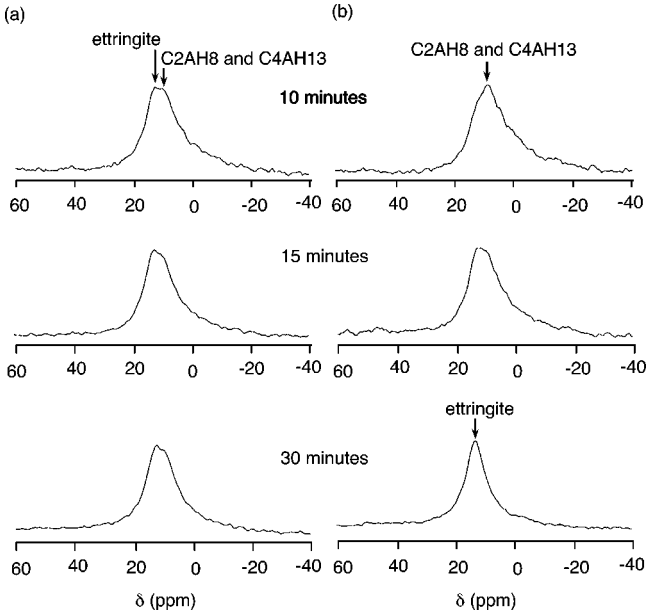

Figure 13. ^{27}Al MAS NMR spectra of C3A (0.6 g) and gypsum (0.4 g) hydrated for 10, 15, and 30 min, (a) with H_6ntmp (1.5 wt %) and (b) without H_6ntmp, showing the rapid but incomplete formation of ettringite ($\delta = 13$ ppm) in the presence of the "retarder" H_6ntmp.

SEM images of partially hydrated C4AF show an aluminate foil forms at the surface of C4AF particles, which closely resembles the early hydration of C3A. SEM also clearly shows the development of ettringite from C4AF pastes hydrated with gypsum. C4AF hydration in the presence of H_6ntmp was followed by SEM. C4AF hydrated for 6.5 h in the presence of H_6ntmp contains smooth particles that are not connected. C4AF hydration, in the presence of gypsum, results in the formation of ettringite is confirmed by SEM (Figure 14a) and XRD. In contrast, in the presence of H_6ntmp the C4AF particles appear to have a thin, amorphous coating and contain platelike angular shapes that appear to have the same coating (Figure 14b). In summary, the addition of H_6ntmp to C4AF completely inhibits hydration, even in the presence of gypsum.

Cement Hydration in the Presence of H_6ntmp. The hydration of cement is obviously far more complex than the sum of the hydration reactions of the individual minerals. Figure 1 depicts a typical cement grain, showing the larger silicate particles surrounded by the much smaller C3A and C4AF particles. The setting of cement can be broken down into several distinct periods. The more reactive aluminate and ferrite phases react first, and these reactions dramatically affect the hydration of the silicate phase. Scrivener and Pratt used TEM

(29) (a) Zakowsky, N.; Wheatley, P. S.; Bull, I.; Attfield, M. P.; Morris, R. E. *Dalton Trans.* **2001**, 2899. (b) Edgar, M.; Carter, V. J.; Grewal, P.; Sawers, L.-J.; Sastre, E.; Tunstall, D. P.; Cox, P. A.; Lightfoot, P.; Wright, P. A. *Chem. Mater.* **2002**, *14*, 3432.

(30) The rapid formation of ettringite with the dudration of C3A and gypsum in the presence of H_6ntmp is confirmed by XRD.

(31) This difference in hydration rate may be due to the fact that iron is not as free to migrate in the pastes as aluminum, which may cause the formation of a less permeable iron-rich layer at the surface of the C4AF particles and isolated regions of iron hydroxide. (a) Mehta, S.; Jones, R.; Caveny, B.; Chatterji, J.; McPherson, G. *Environmental Scanning Electron Microscope (ESEM) examination of individually hydrated Portland Cement phases*; Halliburton Research Center: Duncan, OK. (b) Taylor, H. F. W.; Newbury, D. E. *Cem. Concr. Res.* **1984**, *14*, 565.

(32) Ramachandran, V. S. *Concrete Admixtures Handbook, 2nd Edition*; Noyes Publications: Park Ridge, NJ, 1995.

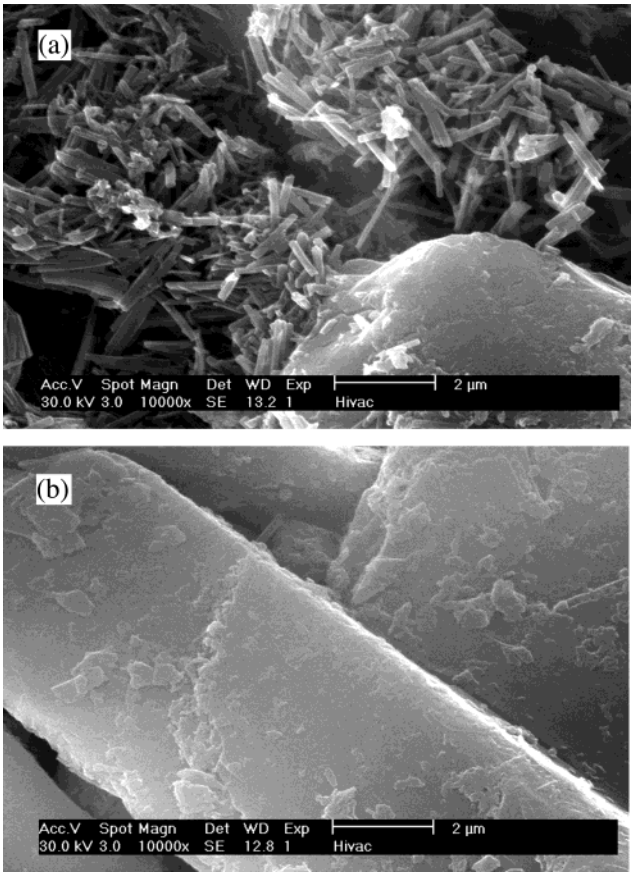

Figure 14. SEM images of C4AF (a) hydrated in the presence of excess gypsum and (b) hydrated in the presence of excess gypsum and H_6ntmp.

to develop the widely accepted model depicted in Figure 15.[33]

In the first few minutes of hydration (Figure 15b), the aluminum and iron phases react with gypsum to form an amorphous gel at the surface of the cement grains and short rods of ettringite grow. After this initial period of reactivity, cement hydration slows down and the induction period begins. After about 3 h of hydration, the induction period ends and the acceleratory period begins. During the period from 3 to 24 h, about 30% of cement reacts to form calcium hydroxide and C−S−H. The development of C−S−H in this period occurs in two phases. After ca. 10 h of hydration (Figure 15c), C3S has produced "outer C−S−H," which grows out from the ettringite rods rather than directly out from the surface of the C3S particles. Therefore, in the initial phase of the reaction, the silicate ions must migrate through the aluminum- and iron-rich phase to form the C−S−H. In the latter part of the acceleratory period, after 18 h of hydration, C3A continues to react with gypsum, forming longer ettringite rods (Figure 15d). This network of ettringite and C−S−H appears to form a "hydrating shell" about 1 μm from the surface of anhydrous C3S. A small amount of "inner C−S−H" forms inside this shell. After 1−3 days of hydration, reactions slow and the deceleratory period begins (Figure 15e). C3A reacts with ettringite to form some monosulfate. "Inner C−S−H" continues to grow near the C3S surface, narrowing the 1-μm gap between the "hydrating shell" and anhydrous C3S. The rate of hydration is likely to depend on the diffusion rate of water or ions to the anhydrous surface. After 2 weeks of hydration (Figure 15f), the gap between the "hydrating shell" and the grain is completely filled with C−S−H. The original, "outer C−S−H" becomes more fibrous.

Cement hydration can be monitored by ^{29}Si MAS, albeit with lower resolution than the pure C3S pastes due to the presence of additional silicate phases (C2S) and paramagnetic iron-containing minerals. A comparison of the spectra in Figure 16 reveals extensive C−S−H formation ($\delta = -78$ ppm) during the first day of hydration. This should be compared to Figure 8, which shows the hydration of the pure C3S paste. In contrast, cement hydrated for 12 days with H_6ntmp (1.5 wt %) reveals only a small amount of C−S−H formation, as indicated by the shoulder at −78 ppm (Figure 16c). It is the early reactions in the hydration of cement that are crucial to controlling the length of the induction period. By the time a significant amount of C−S−H has been formed and can be seen by the emergence of a peak at −78 ppm in the ^{29}Si MAS NMR (i.e., Figure 16b), the induction period is over. Thus, with regard to the silicate phases, the addition of H_6ntmp results in the significant retardation of the hydration process, in particular through the inhibition of the induction period.

^{27}Al MAS NMR can be used to monitor cement hydration. Unhydrated cement shows only 1 peak at 78 ppm, due to the tetrahedral aluminum in C4AF (Figure 17a), since the tetrahedral aluminum centers in C3A are too distorted for observation on a 200-MHz spectrometer. During hydration, the observed peak transforms to that of the octahedral calcium aluminate phases (including C3AH6; $\delta = 11$ ppm); see Figure 17b. This transition from tetrahedral aluminum (ca. 80 ppm) to octahedral aluminum near (ca. 11 ppm) can be used to estimate the extent of cement hydration. In cement pastes hydrated without inhibitors, the transformation to the octahedral calcium aluminate phases is complete well before the end of 2 weeks. Cement hydration with H_6ntmp is severely inhibited, and only a fraction of the total aluminum content has been hydrated even after 2 weeks (Figure 17c). The addition of H_6ntmp does not totally shut down the hydration of the aluminum containing minerals, as occurs for C3S, but the hydration rate is clearly much reduced.

^{31}P MAS NMR of cement hydrated with H_6ntmp (1 wt %) reveals two broad peaks near $\delta = 18$ and 4 ppm due to the terminal (**II**) and bridging (**III**) phosphonate moieties, respectively (Figure 18a). Under these conditions the ratio of terminal (**II**) and bridging (**III**) phosphonate is approximately 2:1. This is the inverse of that found in crystalline $[Ca(H_4ntmp)(H_2O)]_\infty$. The ratio of these peaks is dependent on the exact hydration conditions.

A sample of cement was first hydrated for 2 min without H_6ntmp to allow initial hydration of the aluminate phases, and then H_6ntmp (1 wt %) was added along with additional water. This delayed addition of the inhibitor is actually a common practice in the oil well cementing industry, as many retarders are found to retard cement for longer with delayed addition. The resulting spectrum reveals that more of the bridging

(33) Scrivener, K. L.; Pratt, P. L. *Mater. Res. Soc. Symp. Proc.* **1984**, *31*, 351.

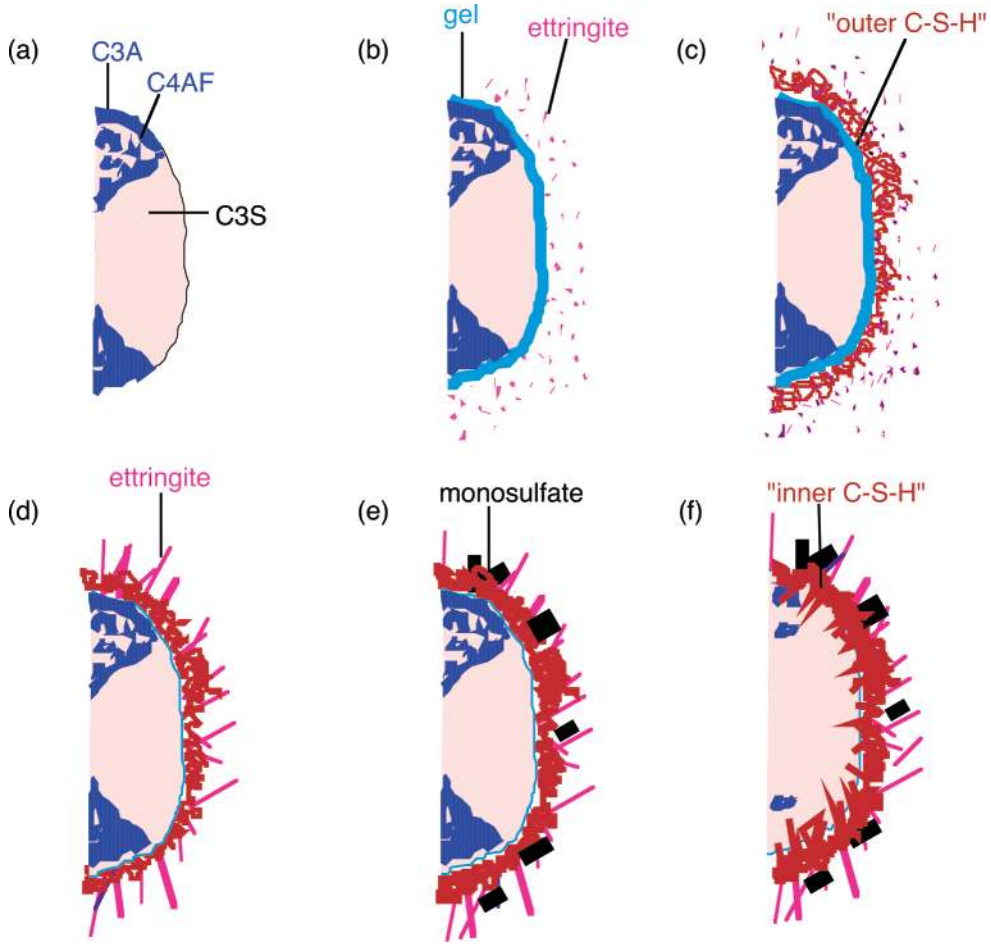

Figure 15. Schematic representation of anhydrous cement (a) and the effect of hydration after (b) 10 min, (c) 10 h, (d) 18 h, (e) 1−3 days, and (f) 2 weeks (Adapted from K. L. Scrivener, Ph.D. Thesis, University of London, 1984).

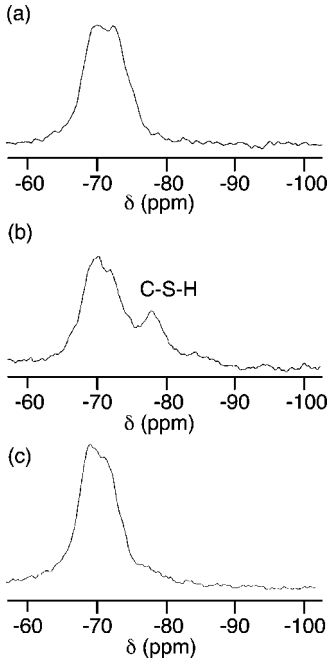

Figure 16. ^{29}Si MAS NMR of (a) dry Class H Portland Cement, (b) after hydration for 24 h, and (c) after hydration for 12 days in the presence of H_6ntmp (1.5 wt %).

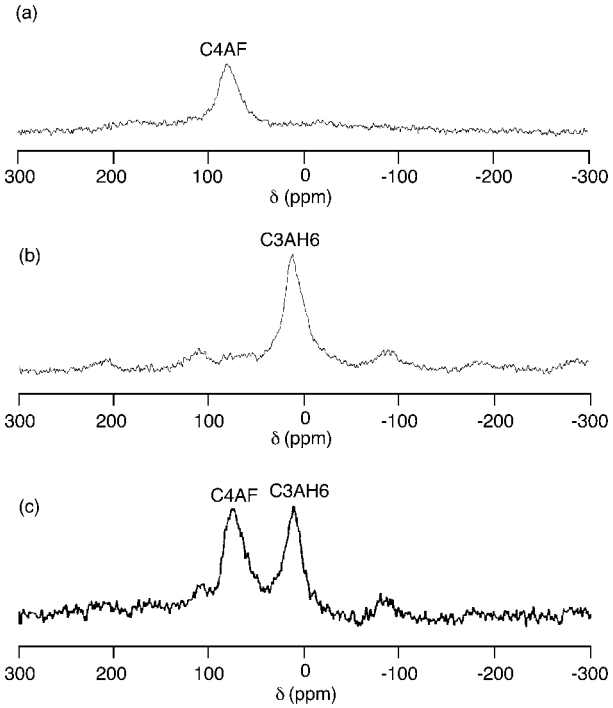

Figure 17. ^{27}Al MAS NMR (52.1 MHz) of (a) anhydrous cement, (b) cement hydrated for 2 weeks, and (c) a sample hydrated for 2 weeks in the presence of H_6ntmp (0.5 wt %).

phosphonate species formed (Figure 18b). The phosphonic acid, H_6ntmp, is known to be a very active retarder at very low weight percentages, ca. 0.1−0.3%. Therefore, a third cement sample was hydrated with less H_6ntmp (0.3 wt %), and the spectrum reveals that the ratio of

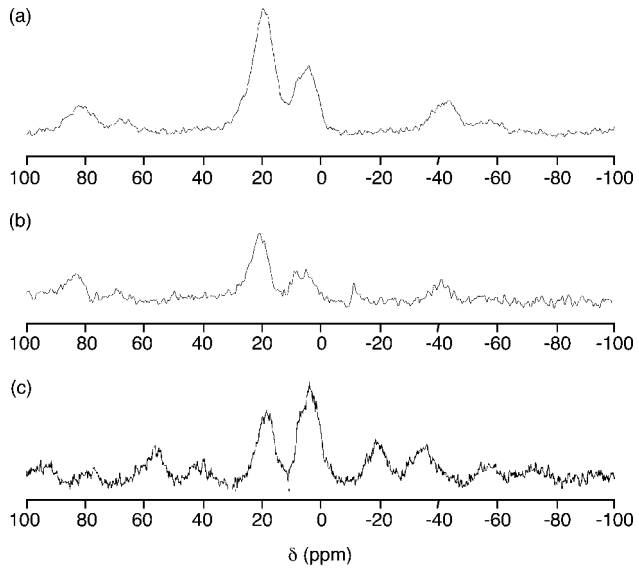

Figure 18. ^{31}P MAS NMR spectra of cement hydrated with (a) 1.0 wt % H_6ntmp, (b) delayed addition of 1.0 wt % H_6ntmp, and (c) 0.3 wt % H_6ntmp.

terminal to bridging phosphonates (Figure 18c) is similar to that found in crystalline $[Ca(H_4ntmp)(H_2O)]_\infty$ (Figure 7).

Because the low concentration and delayed addition conditions are those under which the phosphonic acid is known to be more active, Figure 18c should more accurately reflect the speciation in the field. On the basis of ^{31}P NMR data, we propose that a phosponate complex (or series of complexes) with a structure not unlike that of $[Ca(H_4ntmp)(H_2O)]_\infty$ is most likely responsible for the retardation of cement setting. Furthermore, since the delayed addition of the phosphonic acid allows for some C3A and C4AF to react with gypsum to form ettringite and the amorphous gel at the surface of the cement grains, this material may direct the heterogeneous precipitation of the active calcium phosphonate creating a coating, retarding further hydration.

SEM may be used to observe the surface morphology during hydration. Anhydrous cement grains appear smooth and relatively featureless, with particles ranging in size from ca. 1−50 μm. After hydration, C−S−H appears as a coating on the grains with some characteristic C−S−H rodlike regions and some small crystals of calcium hydroxide present.

XPS analysis of cement hydrated with H_6ntmp reveals almost no aluminum at the surface of the grains. The Ca:Al ratio increases from 15:1 for the anhydrous sample to 78:1 for the sample hydrated with H_6ntmp. This should be compared to the Ca:Al ratio of 25:1 observed for the cement sample hydrated without H_6ntmp. In addition, the Ca:Si ratio is 3.8:1, exactly twice the ratio of 1.9:1 found for cement hydrated without inhibitors. The amount of H_6ntmp used (2.5% relative to the weight of cement) results in a Ca:P ratio of 2:1. Thus, in the presence of H_6ntmp the surface of hydrated cement grains is rich in calcium and phosphorus, and deficient in silicon and aluminum, consistent with the formation of a calcium phosphonate coating.

The extra calcium found at the surface supports a dissolution/reprecipitation mechanism (see below), whereby the H_6ntmp promotes the dissolution of calcium from the mineral phases and then reprecipitates a Ca phosphonate species onto the surface of the hydrating grains.

Conclusions

The reaction of H_6ntmp with calcium salts results in the initial formation of soluble $[Ca(H_nntmp)]^{(4-n)-}$, which precipitate over time as $[Ca(H_4ntmp)(H_2O)]_\infty$. The ratio of bridging to terminal phosphonate groups is dependent on the pH (terminal phosphonate groups increase with increased pH) and the calcium content ($[Ca_3(ntmp)]$ is formed at high Ca:H_6ntmp ratios).

For the hydration of C3S in the presence of the phosphonic acid, ^{29}Si NMR indicates that no C−S−H forms, while XPS reveals a Ca:Si ratio begins Si-rich and then changes to Ca-rich, and ^{31}P MAS NMR reveals that the paste contains various calcium phosphonates. For the hydration of C3A in the presence of H_6ntmp, ^{27}Al MAS NMR reveals that the hydration of C3A is severely inhibited; ^{31}P MAS NMR data indicates that the H_6ntmp is reacting primarily with calcium as opposed to aluminum; and XPS data reveal that a Ca−P-rich layer buries the aluminum at the surface of C3A. H_6ntmp enhances calcium solubility, promoting the dissolution of calcium from anhydrous mineral phases and forming a metastable soluble calcium phosphonate species. However, once formed, the Ca−P complexes are not very soluble and precipitate almost immediately in basic solutions. Precipitation of these complexes forms a layer on top of the hydrating C3A particles, burying the aluminum-rich layer, creating a higher Ca:Al ratio at the surface. For the hydration of C3A in the presence of H_6ntmp and excess gypsum, (a) ^{27}Al MAS NMR shows fast initial formation of ettringite accompanied by another hydrated calcium aluminate (most probably C2AH8 and C4AH13), followed by a period of very slow reactivity in which more ettringite slowly forms; (b) ^{31}P MAS NMR reveals that less of the species at 19 ppm is formed relative to pastes hydrated without gypsum, [Ca(H_4ntmp)] may be present, and some H_6ntmp may be coordinated to aluminum. It has been proposed that the phosphonic acids inhibited the transformation of gelatinous ettringite to crystalline ettringite by adsorbing onto the surface of the grains.[9] On the basis of the foregoing, such a mechanism is not likely since H_6ntmp appears to catalyze, rather than inhibit, the formation of ettringite.

For cement hydration with H_6ntmp, (a) ^{27}Al MAS NMR shows that only half of the aluminum has been converted to the hydrated, octahedral form after 2 weeks; (b) ^{29}Si MAS NMR and SEM reveal that no C−S−H is formed, although some ettringite is formed; (c) ^{31}P MAS NMR shows that H_6ntmp prefers to complex calcium, and it is likely that [Ca(H_4ntmp)] is formed; (d) XPS reveals that a Ca- and P-rich layer forms, burying the aluminum.

Dissolution/Reprecipitation: An Alternative Mechanism for Cement Hydration Inhibition. There are four primary models for cement hydration inhibition: calcium complexation, nucleation poisoning, surface adsorption, and protective coating/osmotic bursting.[1]

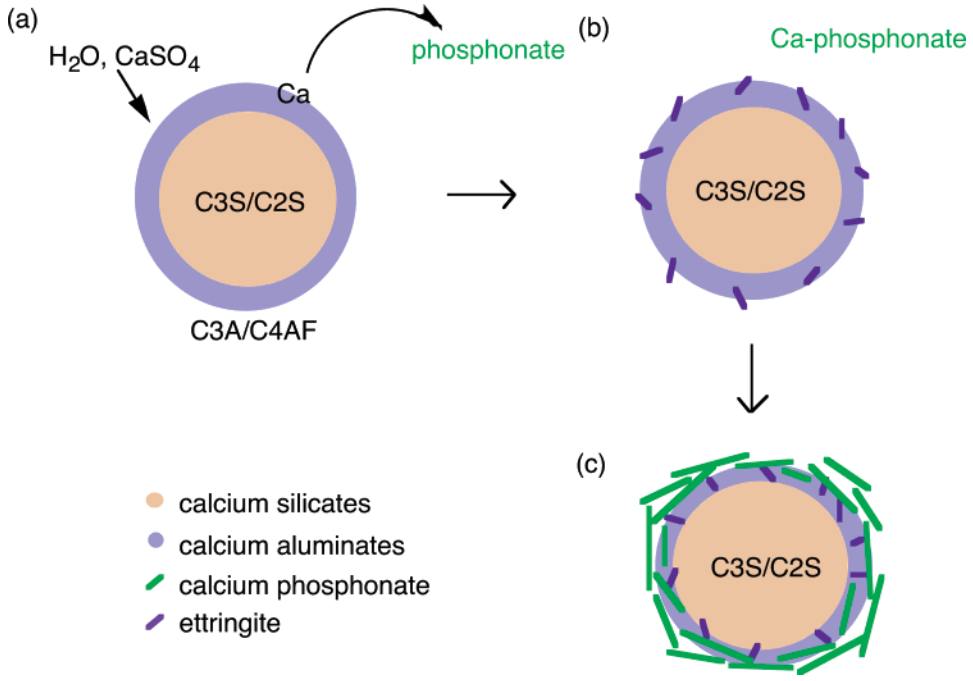

Figure 19. Schematic representation of the H_6ntmp inhibition of cement showing (a) the phosphonic acid promoting calcium dissolution, allowing water and gypsum to react with the aluminum phases at the surface of the cement grain, (b) the formation of a metastable calcium phosphonate, which precipitates onto the hydrating Al surfaces (c), forming a barrier to water and sulfate diffusion.

Calcium complexation involves either removing calcium from solution by forming insoluble salts or chelating calcium in solution to prevent C−S−H formation.[34] However, if the retarder were acting solely by calcium complexation, then one molecule of retarder would be required per calcium ion in solution, and good inhibitors are used in much smaller quantities, on the order of 0.1−2 wt % of cement. In addition, there is no simple correlation between either calcium binding strength or calcium salt solubility and retarding ability.[35] Yet it has been shown that, in pure systems, that is, of C3S and C2S, the lime concentration in solutions is the most important factor in determining the precipitation of C−S−H.[36] Therefore, although calcium complexation must play some role in inhibition, other mechanisms of inhibition must be at work as well.

Inhibition by nucleation poisoning is where the retarder blocks the growth of C−S−H or $Ca(OH)_2$ crystals through inhibiting agglomerates of calcium ions from forming the necessary nucleites. Nucleation inhibitors act on the surface of small clusters; therefore, less than one molecule of retarder per calcium ion is required to produce dramatic results.[37] In a related manner, surface adsorption of inhibitors directly onto the surface of either the anhydrous or (more likely) the partially hydrated mineral surfaces blocks future reactions with water.

The final possible mechanism for hydration inhibition was originally posited to explain the existence of the induction period in C3S and cement hydration in the absence of retarders; however, it may be applied to inhibition in general. In this mechanism, a semipermeable layer at the surface of the cement grain forms and slows down the migration of water and lengthens the induction period. Osmosis will drive water through the semipermeable membrane toward the unhydrated mineral, and eventually the flow of water creates higher pressure inside the protective coating and the layer bursts. Hydration is then allowed to continue at a normal rate.[38] This final mechanism is undoubtedly the mechanism by materials such as ligosulfate operate.

The ability of phosphonic acid retarders to act simultaneously in several different capacities would explain their increased efficiency over more conventional retarders. On the basis of the foregoing results, a new model of hydration inhibition is shown in Figure 19. In this model, cement is modeled as a large calcium silicate particle in a C3A/C4AF matrix. Upon hydration, H_6ntmp first promotes the dissolution of calcium, creating a metastable soluble Ca phosphonate complex and allowing water and gypsum to attack the aluminum at the surface of the cement grains and form ettringite.

The phosphonic acid does not act by simple calcium complexation. If this were the case, then a far greater amount of H_6ntmp would be necessary to produce the same dramatic results that are observed when H_6ntmp is used to inhibit cement hydration. On the basis of our investigation of the reaction of H_6ntmp with various soluble calcium salts, we propose that the Ca phosphonate complex then undergoes a rearrangement (perhaps as shown in Figure 20) and precipitates onto the partially hydrated surfaces. It is possible that the calcium phosphonates prefer to precipitate directly onto the hydrating mineral phases, thereby blocking future

(34) Ramachandran, V. S.; Feldman, R.; Beaudoin, J. *Concrete Science: Treatise on Current Research*; Heyden and Son. Ltd.: Philadelphia, 1981.
(35) Young, J. F. *Cem. Concr. Res.* **1961**, *2*, 415.
(36) Garrault-Gauffinet, S.; Nonat, A. *J. Cryst. Growth* **1999**, *200*, 565.
(37) Thomas, N.; Birchall, J. *Cem. Concr. Res.* **1983**, *13*, 830.
(38) Double, D. *Philos. Trans. R. Soc. London* **1983**, *A30*, 53.

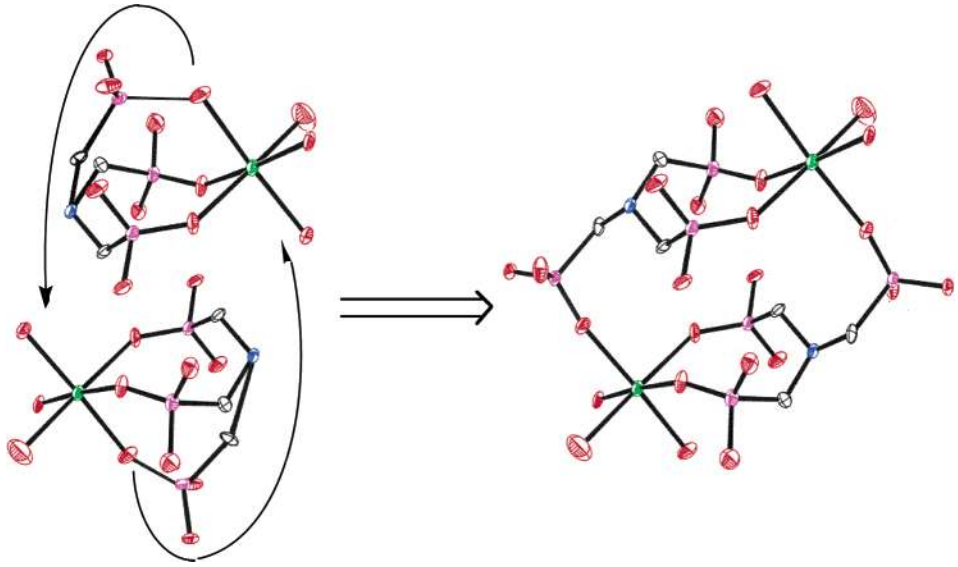

Figure 20. Simulated *fac*-chelate structure (left) may form in aqueous solutions by the complexation of calcium by H_6ntmp and then rearrange to give the bis-chelate calcium dimer (right) that is the structural subunit in $[Ca(H_4ntmp)(H_2O)]_\infty$.

reactions of these phases with water. Heterogeneous precipitation of $[Ca(H_4ntmp)(H_2O)]_\infty$ onto the surfaces of hydrating minerals, as opposed to homogeneous crystal growth, would be enhanced by the ability of terminal phosphonate moieties on the $[Ca(H_4ntmp)(H_2O)]_\infty$ oligomer to bind to the partially hydrated surfaces. Terminal phosphonate moieties, and hence strong attraction to aluminum surfaces, should exist in many calcium phosphonate structures, and hence in general promote heterogeneous crystallization.

If present on the surface of the hydrating grains, the layered sheetlike coating of $[Ca(H_4ntmp)(H_2O)]_\infty$ (Figure 4) would inhibit both further dissolution of calcium and diffusion of water through to the mineral surface. Furthermore, the O···O distances between adjacent uncoordinated phosphonate oxygens on the face of the $[Ca(H_4ntmp)(H_2O)]_\infty$ sheets (8.47 and 9.60 Å) are close to the value proposed by Coveney and co-workers[10] to be the optimum binding distance for the inhibition of ettringite growth.

We propose that the mechanism by which H_6ntmp inhibits cement hydration consists of two steps: First, dissolution, whereby calcium is extracted from the surface of the cement grains, exposing the aluminum-rich surface to enhanced hydration; second, precipitation, whereby the soluble calcium phosphonate oligomerizes either in solution or on the hydrate surface to form an insoluble polymeric Ca phosphonate. The Ca phosphonate binds to the surface of the cement grains, inhibiting further hydration by acting as a diffusion barrier to water as well as a nucleation inhibitor.

Acknowledgment. Financial support for this work was provided by Halliburton Energy Services. The Bruker CCD Smart System Diffractometer of the Texas Center for Crystallography at Rice University was purchased with funds from the Robert A. Welch Foundation. The Bruker Avance 200 and 500 NMR spectrometers were purchased with funds from ONR Grant N00014-96-1-1146 and NSF Grant CHE-9708978, respectively.

Supporting Information Available: X-ray crystallographic data for $[Ca(H_4ntmp)(H_2O)]_\infty \cdot 3.5(H_2O)$] and selected NMR and SEM images (PDF). This material is available free of charge via the Internet at http://pubs.acs.org.

CM0302431